Research Article

The Journal of Comparative Neurology
Research in Systems Neuroscience
DOI 10.1002/cne.24330

Tangential migration of corridor guidepost neurons contributes to anxiety circuits

Andrea Tinterri[1,2,5,6], Marie Deck[1,2], Maryama Keita[1,2], Caroline Mailhes[1,3], Anna Noren Rubin[4°], Nicoletta Kessaris[4], Ludmilla Lokmane[1,2], Franck Bielle[1,2,6*] and Sonia Garel[1,2,7*]

[1]IBENS, Département de Biologie, École normale supérieure, CNRS, Inserm, PSL Research University, F–75005 Paris, France.

[2]Brain Development and Plasticity Team

[3]Acute transgenesis Facility

[4]University College of London, Wolfson Institute for Biomedical Research, Department of Cell and Developmental Biology, London, United Kingdom

[5]Boehringer Ingelheim Fonds, Foundation for Basic Research in Medicine, Schusterstr. 46-48, 55116 Mainz, Germany.

[6]AP-HP, Hôpitaux Universitaires Pitié-Salpêtrière Charles Foix, Service de Neuropathologie, Paris, France.

[7]Ecole de Neurosciences de Paris-Ile de France, 15 rue de l'Ecole de Médicine, 75006 Paris, France.

°Present address: Department of Psychiatry and the Nina Ireland Laboratory of Developmental Neurobiology, University of California San Francisco, CA 94158, USA

*These authors contributed equally to the work.

Correspondence: Sonia Garel garel@biologie.ens.fr (+33-1-44-3237 18)

Institut de Biologie de l'ENS (IBENS), 46 rue d'Ulm, F–75005 Paris, France

Keywords: guidepost cells, corridor neurons, Central extended amygdala, BNST, tangential migration, Ebf1, Islet1, forebrain development, RRID:AB_11142529, RRID:AB_2618776, RRID:IMSR_JAX:024242, RRID:MMRRC_000230-UNC, RRID:MGI:4840402.

Received: Jul 27, 2017; Revised: Aug 31, 2017; Accepted: Sep 01, 2017

Abstract

In mammals, thalamic axons are guided internally towards their neocortical target by corridor (Co) neurons that act as axonal guideposts. The existence of Co-like neurons in non-mammalian species, in which thalamic axons do not grow internally, raised the possibility that Co cells might have an ancestral role. Here, we investigated the contribution of corridor (Co) cells to mature brain circuits using a combination of genetic fate-mapping and assays in mice. We unexpectedly found that Co neurons contribute to striatal-like projection neurons in the central extended amygdala. In particular, Co-like neurons participate in specific nuclei of the bed nucleus of the stria terminalis (BNST), which plays essential roles in anxiety circuits. Our study shows that Co neurons possess an evolutionary conserved role in anxiety circuits independently from an acquired guidepost function. It furthermore highlights that neurons can have multiple sequential functions during brain wiring and supports a general role of tangential migration in the building of subpallial circuits.

Introduction

Brain functioning relies on exquisite circuits that begin to be established during embryogenesis by the coordinated migration of specific neuronal types and their wiring via long-range axonal connections. Crucially, cell migration and axon guidance occur concomitantly, influencing each other in a complex developmental choreography that is not yet fully understood. In particular, the mammalian neocortex forms connections with the rest of the brain via the internal capsule, a large fascicle of axons that comprises corticofugal efferent and reciprocal thalamocortical afferent projections (TCAs), which convey sensory and motor information to the neocortex (Grant, Hoerder-Suabedissen, & Molnár, 2012; Lemon, 2008; Molnár, Garel, López-Bendito, Maness, & Price, 2012; Sherman, 2016). The guidance of TCAs along an internal trajectory relies on a population of tangentially migrating neurons called corridor (Co) cells, which form a permissive “bridge” for axons *en route* to the neocortex (Bielle, Marcos-Mondejar, et al., 2011; Feng et al., 2016; Lokmane et al., 2013; Lokmane & Garel, 2014; Squarzoni, Thion, & Garel, 2015; Zhou, Qu, Tissir, & Goffinet, 2009). Co cells are located in the subpallium, which is a major site of neuronal proliferation and migration. The subpallium includes the lateral, medial and caudal ganglionic eminences (LGE, MGE and CGE, respectively) and the preoptic area (POA); these structures generate projection neurons of the striatum, the pallidum and the amygdala (Dodson et al., 2015; Eisenstat et al., 1999; Hagimoto, Takami, Murakami, & Tanabe, 2017; Hamasaki, Goto, Nishikawa, & Ushio, 2003; Long, Cobos, Potter, & Rubenstein, 2009; Marín &

Rubenstein, 2003; Nóbrega-Pereira et al., 2010; Waclaw, Ehrman, Pierani, & Campbell, 2010; Wichterle, Turnbull, Nery, Fishell, & Alvarez-Buylla, 2001). In addition, the MGE, the LGE/CGE and POA produce interneurons that migrate tangentially to contribute to cortical and subcortical circuits (J. G. Corbin, Nery, & Fishell, 2001; Joshua G. Corbin & Butt, 2011; Elshatory & Gan, 2008; Gelman, Marín;, & Rubenstein, 2012; Hirata et al., 2009; Marin, Anderson, & Rubenstein, 2000; Marín & Rubenstein, 2001; Nóbrega-Pereira et al., 2008; Torigoe, Yamauchi, Kimura, Uemura, & Murakami, 2016; Touzot, Ruiz-Reig, Vitalis, & Studer, 2016; Xu, Tam, & Anderson, 2008). Co cells express transcription factors *Islet1* and *Ebf1* (López-Bendito et al., 2006), similarly to LGE-derived striatal projection neurons of the direct pathway (dSPN; Ehrman et al., 2013; Garel, Marín, Grosschedl, & Charnay, 1999; Lu, Evans, Hirano, & Liu, 2014). However, unlike the latter, which migrate radially to form the striatum (Halliday & Cepko, 1992; Hamasaki et al., 2003; Wichterle et al., 2001), Co neurons migrate tangentially from the LGE into the MGE from E11.5 to E14, where they create a permissive corridor for TCAs in the otherwise non-permissive MGE (López-Bendito et al., 2006). It has been shown that defects in corridor positioning led to abnormal TCAs pathfinding (Bielle, Marcos-Mondejar, et al., 2011; Feng et al., 2016; Morello et al., 2015; Zhou et al., 2009). In addition, Co cells not only control TCA internal navigation but also their topographic organization. Indeed, Co cells express gradients of guidance cues that organize TCAs along the rostro-caudal axis and allow them to target specific cortical areas (Bielle, Marcos-Mondéjar, et al., 2011; Garel & López-Bendito, 2014; Lokmane et al., 2013; Lokmane & Garel, 2014; Squarzoni et al., 2015). Therefore, Co cells play essential and diverse roles in TCA pathfinding

(Lokmane & Garel, 2014; López-Bendito et al., 2006; Molnár et al., 2012; Squarzoni et al., 2015). Despite their importance, we have little information on this neuronal population and whether it contributes to adult brain circuits. Evidence from other guidepost populations in the brain, such as the lateral olfactory tract cells (de Frutos et al., 2016), suggest that guidepost neurons can have additional roles in brain circuit function (Squarzoni et al., 2015). Furthermore, an independent role for Co cells is supported by evolutionary developmental studies. Indeed, even though the internal capsule is only present in mammals, cells with a molecular identity similar to Co cells have been also identified in avian and reptile embryos (Bielle, Marcos-Mondejar, et al., 2011; Bupesh, Abellán, & Medina, 2011). Moreover, gene expression studies suggest contribution of LGE derivatives to the central and extended amygdala, evolutionarily conserved superstructures located in the subpallium that contain neurons of different developmental origin and are involved in fear and anxiety control (Hott et al., 2016; Ranjan et al., 2017) and anxiety (Geng et al., 2016; Morano, Bailey, Cahill, & Dumont, 2008; Ventura-Silva et al., 2012). These observations raised the intriguing possibility that guidepost might be an acquired function for Co cells, which would have a distinct, evolutionary conserved role.

Here, we provide evidence that LGE/CGE derived Co projection neurons contribute to specific subdivisions of the bed nucleus of the stria terminalis (BNST), a key structure of the extended amygdala. We first show that the LGE/CGE generates the Co and a ventromedial stream (Vms), two tangential paths in the MGE territory, which include Co neurons and striatal-like *Drd2-EGFP*$^{+}$ neurons. We define Co/Vms neuron molecular fingerprint and use it to

show their contribution to different nuclei of the central extended amygdala in late embryonic and postnatal brain. Consistently, we show that in *Ebf1* conditional knockout mice, in which Co neuron migration is affected at early stages, the BNST is reduced postnatally. Overall, our work shows that Co neurons are not transient actors in brain wiring but could possess an evolutionary conserved role in fear and anxiety related networks that is independent from their acquired guidepost function. More generally, our work sheds new light on the relationship between tangential migration in the subpallium and the formation of forebrain circuits.

Material and methods

Mouse lines

For fate mapping studies, *Islet1*$^{Cre/+}$ (RRID:IMSR_JAX:024242) and *Nkx2.1cre* animals (RRID:IMSR_JAX:008661; Srinivas et al., 2001; Xu et al., 2008), were crossed with either *R26*$^{LacZ/LacZ}$, *R26*$^{YFP/YFP}$ or *R26*$^{mt/mt}$*;Drd2-EGFP* mice. *Nkx2.1cre*;*Dlx1*$^{fl\text{-}VENUS\text{-}fl}$ (RRID:MGI:4840402) E14 and E18.5 embryos were kindly provided by N. Kessaris and generated as described in (Rubin et al., 2010). *Dlx5/6::Cre;Ebf1*$^{fl/-}$ mice (Lokmane et al., 2013) were obtained by crossing *Dlx5/6::Cre* (RRID:IMSR_JAX:023724; Zerucha et al., 2000) mice with *Ebf1*$^{+/-}$ to generate *Dlx5/6::Cre;Ebf1*$^{+/-}$ animals, which were in turn backcrossed with *Ebf1*$^{fl/fl}$ mice. Heterozygous embryos did not show any phenotype and were used as controls. Wild-type mice were used for expression analysis, cholera toxin injection and DiI labelling experiments. All transgenic lines are kept in C57/Bl6 background, with the exception of *Islet1*$^{Cre/+}$ and *Drd2-EGFP* (RRID:MMRRC_000230-UNC; Gong et al., 2003) lines that are kept in B6D2F1/J background. The day of vaginal plug was considered as embryonic day (E) 0.5 and day of birth as postnatal day (P) 0. Animals were kept under French and EU regulations, following recommendations of the local ethics committee.

In situ hybridization, immunohistochemistry and X-Gal staining

For *in situ* hybridization, brains were fixed overnight in 4% paraformaldehyde in PBS (PFA) at 4°C. 80 to 100µm-thick free-floating vibratome sections (Leica S1000) were hybridized as described (Lokmane et al., 2013). For immunohistochemistry, embryos were collected in cold PBS1X, their brains were dissected and post-fixed in 4% in PFA for 2 (E13.5-E14.5) or 8 (E17.5-E18.5) hours. Postnatal mice were perfused with 4% PFA. Brains were

dissected and post-fixed overnight at 4°C. Immunohistochemistry was performed on 60µm free-floating vibratome sections. Slices were incubated 1h at room temperature (RT) in a blocking solution containing 0,25% Triton X-100 (Sigma), 0,02% Gelatine in PBS, and incubated in the same blocking solution with primary antibodies overnight at 4°C. Hoechst (Sigma) was used for fluorescent nuclear counterstaining. For X-gal staining, brains or cultures vesicles were fixed in 4% PFA at 4°C for 40 min, washed in PBS and incubated with X-gal staining solution (10 mM Tris-HCl pH7.3, 0.005% Na-desoxycolate, 0.01% Nonidet P40, 5 mM $K_4Fe(CN)_6$, 5 mM $K_3Fe(CN)_6$, 2 mM $MgCl_2$ and 0.8 mg/ml X-gal) at 37ºC until the staining was visible. After several PBS washes, brains were post-fixed in 4% PFA overnight.

EdU staining

Pregnant dams were intraperitoneally injected at the appropriate gestation day with a solution containing 5-Ethynyl-2'-deoxyuridine (EdU, Thermo Fisher). 60-100µm-thick free-floating vibratome sections were processed following manufacturer instructions (Click-iT EdU Alexa Fluor 488 Imaging kit, Life Technologies) for 30 minutes at RT. Sections were rinsed three times in 3%BSA and then in PBS. Hoechst staining was performed for 30 min at RT before pursuing the immunohistochemistry protocol as described above.

Cholera Toxin tracing

Alexa594 coupled -Cholera Toxin B subunit (CTB, Alexa Fluor) was injected in the thalamic/hypothalamic region of wild-type embryos, that were subsequently maintained in “bubbling” oxygen at 37°C for 3h in a solution containing DMEM-F12 (Invitrogen), Glutamine, Glucose and Pen/Strep. Injected brains were then

fixed by immersion in 4% PFA for 6 hours at 4°C and rinsed several times before pursuing the immunohistochemistry protocol as described before.

Image acquisition, analysis and quantification

Images were acquired with fluorescence binocular microscope (Leica MZ16 F), fluorescent microscope (Leica DM5000 B) or confocal microscope (Leica TCS SP5). Images were then processed with ImageJ and Adobe Photoshop software. For cell density and colocalization analysis, single-plane confocal images were taken in the regions of interest, defined using anatomical landmarks, in at least three different animals for each condition. Cell counting was performed semi-automatically using built-in functions in ImageJ. For each experiment, sample images were manually counted to double-check the quality of semi-automated counting. For area measurement in Figure 6, the dBNST was defined using the anterior commissure as anatomical landmark, while $Ctip2^{+}FoxP2^{+}$ immunostaining was used to help distinguish BNST from striatal territory. Area was measured using ImageJ; three different rostro-caudal planes were measured from each animal (n=10 for controls and 5 for conditional mutants) and averaged.

Statistical analyses

All data are presented as mean ± SD. Two-tailed parametric Student's T test was used to compare two distributions in co-labelling analysis (Figures 2 and 3). Two-tailed non-parametric Mann-Whitney U test was used to compare two distributions in BNST area measurements (Figure 6). All statistical analyses were performed using GraphPad Prism software. P-values are shown as follows: * $p<0.05$, ** $p<0.01$, *** $p<0.001$.

Table of Primary Antibodies:

Antigen	Description of immunogen	Source, host species, catalogue No., clone or lot No., RRID	Concentration
Ctip2	Synthetic peptide conjugated to KLH, residues 850 - 950 of Human Ctip2.	Abcam, Rabbit polyclonal, ab28448, RRID:AB_2049548	1/500; IF
DsRed	Recombinant full-length DsRed-Express, a variant of Discosoma sp. Red fluorescent protein	Clontech, rabbit polyclonal, 632496, RRID:AB_10013483	1/500; IF
Ebf1	Recombinant fragment, corresponding to a region within amino acids 57-317 of Human EBF1.	Abcam, Rabbit polyclonal, ab126135, RRID:AB_11142529	1/250, IF
Islet1	C-terminal residues 178–349 of rat Islet1	Developmental Hybridoma Bank, (Univ. of Iowa, Iowa); mouse monoclonal IgG2b; catalog No. 39.4D5, RRID:AB_2618776	1/100, IF
FoxP1	Synthetic peptide conjugated to KLH , residues 650 to the C-terminus of Human FOXP1	Abcam, Rabbit polyclonal, ab16645, RRID:AB_732428	1/200, IF
FoxP2	Raised against a short peptide, epitope mapping near N-terminus of human FOXP2	Santa Cruz, goat polyclonal, sc-21069, RRID:AB_2107124	1/200, IF
GFP	Recombinant full-length GFP	Abcam, chicken polyclonal, ab13970, RRID:AB_300798	1/1000, IF
Nkx2.1	synthetic peptide corresponding to amino acids 110–122 at the amino terminus of rat NKX2.1	Biopat immunotochnologies, Rabbit polyclonal, PA0100, RRID :AB_2313674	1/1000, IF
Pkc-delta	Recombinant fragment within Mouse PKC delta aa 500 to the C-terminus.	Abcam, Rabbit monoclonal, ab182126, RRID:AB_2172236	1/250, IF

The specificity of the aforementioned antibodies has been previously established (Arlotta et al., 2008; Lokmane et al., 2013; Bielle et al., 2011, 2013; Xu et al., 2008; Cai et al., 2014).

Results

LGE/CGE-derived ventral tangential streams in the subpallium

The Co is defined at embryonic day (E) 13.5 as a region located in the MGE superficially to the globus pallidus that express LGE molecular markers (Bielle, Marcos-Mondejar, et al., 2011; López-Bendito et al., 2006). To unambiguously establish the origin of Co neurons, we took advantage of several fate-mapping models, including subtractive genetic approach (Figure 1). First, we assessed whether Co neurons derive from MGE or preoptic area (POA) progenitors, which express the transcription factor Nkx2.1 (Figures 1a-1d, Xu et al., 2008). We found that *Nk2.1$^{Cre/+}$;R26$^{YFP/+}$* cells populate the MGE and GP at E13.5, but only few scattered YFP^{+} cells are located in the region of the Co (Figure 1b). In addition, these YFP^{+} few cells did not co-express the Co neuron marker Islet1 (Figure 1c), and likely correspond to MGE or POA-derived interneurons migrating in the subpallium and or towards the neocortex (Figure 1d, Brown et al., 2012; Marin, Anderson, & Rubenstein, 2000; Marín & Rubenstein, 2001; Xu, Tam, & Anderson, 2008).

In order to fate map LGE/CGE-derived neurons, we crossed *Nk2.1$^{Cre/+}$* with *Dlx1$^{fl\text{-}venus\text{-}fl}$* mice (Kessaris, Magno, Rubin, & Oliveira, 2014; Rubin et al., 2010). Since *Dlx1* is expressed in precursors of the LGE, MGE and CGE (Eisenstat et al., 1999; Yun et al., 2002), Venus expression is restricted to LGE/CGE-derived cells in *Nk2.1$^{Cre/+}$; Dlx1$^{fl\text{-}venus\text{-}fl}$* embryos (Figures 1e-1g). Venus expression showed that the LGE/CGE gives rise, in addition to populations in the striatum (Halliday & Cepko, 1992; Hamasaki et al., 2003), to Co neurons and another stream that is medial to the striatum and ventral to the GP (ventro-medial

stream, Vms). Taken together, our results indicate that the LGE/CGE generates tangential streams, including the Co (Figure 1h).

To define a more restrictive fate-mapping model, we examined *Islet1*$^{Cre/+}$*; R26*$^{YFP/+}$ mice, since Islet1 is expressed in Co neurons (Figures 1i-j; Ehrman et al., 2013; López-Bendito et al., 2006; Lu et al., 2014). We confirmed that YFP$^+$ cells are bona fide Nkx2.1-negative striatal and Co cells (Figures 1i-i') that co-express Ebf1 (López-Bendito et al., 2006). Collectively, our results indicate that Co neurons derive from the LGE/CGE and are labelled by *Islet1*^{cre} recombination. Notably, the Co domain comprises also cells generated in the Nkx2.1-positive domain (Figure 1c) as well as cells that still express Nkx2.1 (Figure 1i'), which likely correspond to interneurons migrating towards the neocortex or basal ganglia, respectively.

Since the striatum does not only contain Islet1$^+$ and Ebf1$^+$ direct projection neurons (dSPN; Ehrman et al., 2013; Lobo, Karsten, Gray, Geschwind, & Yang, 2006; Lobo, Yeh, & Yang, 2008; Lu et al., 2014) but also *Drd2-EGFP*-expressing indirect projection neurons (iSPN; Gong et al., 2003; Morello et al., 2015), we examined whether the Co and Vms regions contained exclusively dSPN-like neurons. We observed *Drd2-EGFP*+ cells in the Vms and superficial Co at E13.5 (Figure 2a), which expressed Ctip2 (Figures 2b-d) and not Ebf1 (Figures 2e-f). Both populations exhibited bipolar, tangentially oriented morphologies, supporting the hypothesis that these cells migrate tangentially (insets in Figures 2a-a''). *In vivo*, the *Drd2-EGFP*$^+$ population increased at E14.5, alongside with a change in Co shape, getting thinner proximally end and assuming a triangular shape at the ventral end (Figures 2g-h'). The strong co-expression with Ctip2 suggested that *Drd2-EGFP*$^+$ neurons in the Co might be

projection neurons, or iSPN-like neurons, rather than interneurons (Figures 2b-d). To further address this issue, we examined the expression of Nkx2.1 and Prox1, which respectively label interneurons generated by the MGE and LGE/CGE (Miyoshi et al., 2015; Nóbrega-Pereira et al., 2008; Rubin & Kessaris, 2013; Touzot, Ruiz-Reig, Vitalis, & Studer, 2016; Xu et al., 2008) and found no co-labelling with GFP^+ cells (Figures 2i-j). Finally, using grafts in slice co-culture experiments, we observed streams of cells tangentially migrating from the LGE/CGE transplants, from either ubiquitously GFP-expressing embryos or *Drd2-EGFP*+ embryos (Figures 2k-l'). Taken together, our findings indicate that the LGE/CGE generates Co dSPN-like and iSPN-like neurons, which form tangential streams into the MGE territory.

Defining the molecular and cellular identity of Co neurons

Since the expression of Ebf1 and Islet1 is common to Co cells and dSPN of the striatum, we examined whether these two cell types share additional molecular markers. Using E13.5 *Islet1*$^{Cre/+}$*; R26*$^{YFP/+}$ embryos, we confirmed that dSPN were labelled by immunostaining against transcription factors Ctip2 (Figures 3a-d, 93±2%) and FoxP1 (Figures 3e-h; Arlotta, Molyneaux, Jabaudon, Yoshida, & Macklis, 2008; Chen et al., 2016; Chiu et al., 2014; Enard, 2011; Enard et al., 2009; Ferland, Cherry, Preware, Morrisey, & Walsh, 2003; Garcia-Calero, Botella-Lopez, Bahamonde, Perez-Balaguer, & Martinez, 2015). In the Co, most YFP^+ cells expressed Ctip2 (Figure 3c) but almost none co-expressed FoxP1 (Figure 3g) and its homolog FoxP2 (data not shown). This difference allows us to define Co cells as LGE/CGE-derived cells expressing Ctip2 but not FoxP1 (Figures 3d,h). A similar molecular fingerprint characterizes *Islet1*$^{Cre/+}$*; R26*$^{YFP/+}$

cells in the Vms (data not shown). These results indicate that Co and Vms neurons have a common molecular identity that partially differs from dSPN, despite sharing a LGE/CGE origin. These observations raised the possibility that Co neurons might be projection neurons. To test this possibility, we injected fluorescently labelled cholera toxin (CTB) in the hypothalamic/thalamic region of E12.5 embryos (Figures 3i-k). We identified numerous retro-labelled cells in the Co that are positive for Islet1^{+}Ctip2^{+} and negative for Nkx2.1 (Figures 3j-k). In addition, we inserted a DiI crystal in the hypothalamic region at E13 and E14 (Figures 3l-n and data not shown), which retro-labelled several Ebf1^{+} Co neurons (Figures 3m-n). Therefore, Co neurons have a molecular identity of projection neuron and subsets extend axons outside of the subpallium, which might contribute to their guidepost activity on thalamic axons (Squarzoni et al., 2015). Since Co neurons are not expressing Prox1 (Figure 2j), the main molecular marker of LGE/CGE-derived interneurons, our results collectively support that Co cells have a projection neuron identity, which shares common features but is distinct from the one of dSPN.

Co-derived neurons contribute to central extended amygdala

To test whether Co and Vms neurons contribute to brain structures at later stages, we took advantage of our fate-mapping models and defined molecular fingerprints. Using E18.5 *Islet1$^{Cre/+}$; R26$^{LacZ/+}$* (Figures 4a,b), *Islet1$^{Cre/+}$; R26$^{YFP/+}$* (Figures 4c,d), *Nkx2.1cre; R26$^{LacZ/+}$* (Figures 4e,f) and *Nk2.1-cre*; *Dlx1$^{fl\text{-}venus\text{-}fl}$* (Figures 4g,h) we found that the Islet1^{+} LGE/CGE-derived lineage contributed to the bed nucleus of the stria terminalis (BNST) and the interstitial nucleus of posterior limb of anterior commissure (Ipac, Figure 4b). Considering their

relative location, the BNST likely derives from the Co and the Ipac from the Vms (Figures 4a,b). Consistent with this hypothesis, we found that cells in the BNST express *Ebf1* and are born at E11.5 or to a lesser extent at E12.5 (Figures 4i-m). We furthermore found that, like Co and Vms cells, *Islet1*$^{Cre/+}$*; R26*$^{YFP/+}$ labelled neurons in the BNST and Ipac were Ctip2^{+} (Figures 4n-q) and FoxP1^{-} (Figures 4r-u). The BNST and Ipac are part of the central extended amygdala, a continuous macrostructure involved in reward and anxiety, which has previously been proposed to originate in the LGE (Alheid, 2003; Bupesh et al., 2011; J. S. de Olmos & Heimer, 1999; Hirata et al., 2009; J. L. Olmos, Real, Medina, Guirado, & Dávila, 2005; Waclaw et al., 2010; Walker & Davis, 2008; Waraczynski, 2006). Our long-term fate mapping establishes such origin and conversely reveals that Co cells and Vms cells contribute to central extended amygdala structures, namely the BNST and Ipac, respectively. Since the Co and Vms also contained early-born Drd2-EGFP^{+}Ctip2^{+} cells (Figure 1), we searched for their potential derivatives at late embryonic stages and found them in both the BNST and Ipac (Figures 4v-y). Taken together, these findings reveal that LGE/CGE projection neurons forming the Co and Vms contribute to nuclei of the extended amygdala, thereby revealing an intriguing link between thalamic guidepost neurons and central extended amygdala circuits.

Co-derived neurons contribute to nuclei that mediate anxiety response

To further investigate whether Co-derived cells contributed to specific circuits, we focused on their contribution to the BNST, which organization and function has been recently investigated (Asok, Schulkin, & Rosen, 2016; Choi et al., 2007; Daldrup, Lesting, Meuth, Seidenbecher, & Pape, 2016; H. W. Dong,

Petrovich, & Swanson, 2001; Geng et al., 2016; Hott et al., 2016; Kim et al., 2013). The BNST is a complex structure which comprise a large number of subdivisions that are difficult to identify on anatomical criterions (Bayer, 1987; Ju & Han, 1989). However, in its rostral part, it is formed by morphologically discernible subdivisions including the anterodorsal (BNSTad), the ovalis (BNSTov) and the juxtaposed nucleus and dorsomedial (BNSTdm) nuclei (Figure 5a). These subdivisions play distinct roles, as illustrated by the fact that the BNSTad send long-range projections and its activation has anxiolytic effect, whereas the BNSTov inhibits anxiolysis by targeting the BNSTad (H.-W. Dong & Swanson, 2004; Kim et al., 2013). At P5, *Islet1*$^{Cre/+}$*;R26*$^{mt/+}$ (Figure 5b) and *Drd2-EGFP*$^{+}$ (Figure 5b') populate different rostral subdivision of the BNST, but do not overlap (Figures 5b'' and 5b'''), showing that Islet1-cre recombined neurons retain a D2r-negative identity and are mostly observed in different nuclei (Figures 5b-b''). In particular, BNSTov contained a relatively small number of Islet1cre-recombined cells. We thus examined juvenile mice (P14) where BNSTov neurons can be identified by the expression of protein kinase C delta (*Pkcδ*, Figures 5c-g; (Bodnar, 2013; Cai, Haubensak, Anthony, & Anderson, 2014; Haubensak et al., 2010). A large number of Co-derived neurons populated the BNSTad at this stage (Figures 5c-g), whereas very few of them were found within the BNSTov (Figures 5c-g'). By contrast, a large population of *Drd2-EGFP*$^{+}$ was observed in this nucleus compared to the adjacent BNSTad (Figures 5h-k). These findings suggest that LGE/CGE derived neurons that transiently populate the corridor contribute more specifically to the BNSTad and not the BNSTov. Since the BNSTad has been shown to have an anxiolytic effect and the BNSTov an antagonistic one (Ahmari & Dougherty,

2015; Crowley et al., 2016; Geng et al., 2016; Pêgo et al., 2008; Tovote, Fadok, & Lüthi, 2015; Ventura-Silva et al., 2012) Co-derived neurons might play specific functions in reducing anxiety-like behaviour (Figure 5h). Taken together, our findings show that LGE/CGE contributes to the formation of evolutionarily conserved structures of the extended amygdala, which possess specific roles in anxiety-related circuits.

Defective corridor formation lead to reduction in BNST size

To further test if Co derived populations participate to the BNST, we investigated whether defective corridor development could impact BNST formation. To this aim, we compared normal corridor development with a conditional knockout (cKO) line for *Ebf1* (*Dlx5/6::Cre;Ebf1*$^{fl/-}$, Lokmane et al., 2013). Along with defects in striatal formation (Garel et al., 1999; Lobo et al., 2006, 2008), *Ebf1* cKO embryos showed a delayed and abnormal migration of Co neurons, which is accompanied by defects in internal capsule organization (Garel, Yun, Grosschedl, & Rubenstein, 2002; Lokmane et al., 2013). We first confirmed that Ebf1 protein is absent in Co neurons as soon as E13.5 (Figures 6a-b). Furthermore, we performed an *in situ* hybridization timecourse in order to follow Co and Co-derived neuron trajectory across embryonic development (Figures 6c-h). We took advantage of a *Ebf1* full length riboprobe, which allows specific labelling of Co neurons in both control and cKOs by detecting all *Ebf1* transcripts, including the floxed form (Lokmane et al., 2013). We confirmed that Co and Vms shape are already altered at E13.5 (Figures 6c, d) and that this defect persists at E14.5 (Figures 6e, f). At E17.5, *Ebf1* transcript is reduced in the cKO BNST (Figures 6g, h), suggesting a lesser contribution of Co-derived

neurons to this structure due to Co impaired migration. Finally, to test whether this impairment in BNST development was still present at later stages, when *Ebf1* is not expressed anymore (Garel et al., 1999), we measured the area of the BNST at P5 in control and *Ebf1* cKO mice. We found a small but significant reduction of the total BNST size in mutant mice compared to controls (Figures 6i-j), indicating that the developmental defect we observed was not transient but affected BNST morphogenesis also at postnatal stage. Taken together, our findings indicate that defective migration of Co neurons correlates with abnormal BNST morphogenesis, consistently with our fate-mapping studies.

Discussion

We have shown that projection neurons originating from the LGE/CGE form a transient tangential corridor during embryonic development, which contributes to anxiety circuits of the extended amygdala in the mature brain. LGE/CGE derived cells contains two neuronal populations, Co cells and *Drd2-EGFP*$^{+}$ neurons, which bear resemblance in terms of molecular identity to striatal direct and indirect projection neurons, respectively (Figure 7). In contrast to the MGE, whose derivatives can be permanently labelled by Nkx2.1cre tracing (Marin et al., 2000; Xu et al., 2008), there are no ideal tools currently available to specifically fate-map LGE progenitors and their progeny. Through a combination of genetic and immunohistochemistry approaches we established that, in addition to the striatum (Hamasaki et al., 2003; Wichterle et al., 2001), different types of LGE-derived neurons colonize the MGE via tangential streams of migration. Intriguingly, another LGE-derived population deriving from *Ascl1*$^{+}$ progenitors migrates tangentially into the GP, where they become arkypallidal neurons (Dodson et al., 2015; Nóbrega-Pereira et al., 2010). This population expresses FoxP2 (Dodson et al., 2015), but whether they are part of the Islet1 lineage is currently unknown.

In addition to Co neurons, we also found by genetic tracing and migration assays that the LGE/CGE gives rise to another stream of migration, the Vms (Figures 2 and 7). The Vms contains both Islet1-lineage neurons and Drd2-EGFP+ neurons, showing a similar cellular composition to the Co. Whether Vms neurons migrate tangentially like Co cells or along radial glia processes still remains to be determined. Taken together, these findings indicate that, in addition to interneurons (Ciceri et al., 2013; Long et al., 2009; Rubin & Kessaris,

2013; Torigoe et al., 2016), the LGE produces a wide panel of projection neurons that contribute to different structures of the basal ganglia and amygdala (Figure 7). Striatal-like projection neurons are involved in different circuits (dorsal and ventral striatopallidum, extended amygdala and septa-preoptic) which share an organizational framework (Heimer et al 2008). This framework includes (i) cortical inputs, and (ii) outputs via sparsely spine GABAergic neurons to thalamo-cortical reentrant pathways and to autonomic, somatic motor and neuroendocrine effectors in hypothalamus and brainstem. Each circuit is biased toward a functional role (appendicular motor function, motivation, integration of motor behavior and emotional state). Our results show the role of tangential migration to parcimoniously produce from a unique LGE source the striatal-like projections neurons of different functional circuits. They also identify distinct expression of the transcription factors FOXP1 and FOXP2 in neuronal precursors of striatum and extended amygdala. This expression may underlie different functional properties of striatal-like projections neurons in these distinct functional circuits.

Building on previously published study, our work reinforces the idea that complex and orchestrated choreographies of migration are essential for the building of basal ganglia nuclei projection neurons (Figure 7). Our analyses further raise the question of what are the common features among LGE-derivatives and how many different subtypes can be distinguished. For example, a common trait of all subtypes of striatal projection neurons is their spiny morphology, raising the question of whether other striatal-like LGE derivatives possess this property, as is the case for Islet1^{+} neurons of the central amygdala (Waclaw et al., 2010). At postnatal stages, Co-derived neurons and *Drd2-EGFP*$^{+}$ neurons participate to specific nuclei of the BNST, suggesting that they might play distinct and potentially opposite roles in anxiety

circuits. It will be of great interest to dissect whether Co-derived neurons and *Drd2-EGFP*$^{+}$ neurons similarity to striatal dSPN and iSPN extends to electrophysiological and connectivity properties, in terms of reciprocal connectivity (Taverna, Ilijic, & Surmeier, 2008) and input preference (Deng, Wong, Wan, & Reiner, 2014; Reiner, 2010; Sippy, Lapray, Crochet, & Petersen, 2015; Wall, De La Parra, Callaway, & Kreitzer, 2013). Similarly, since the BNST and the central amygdala show similarities in the cellular organization of their circuits, it will be interesting to examine whether dSPN and iSPN like contribute to distinct divisions of this nucleus. This work will shed light on the fine-grain connections that control anxiety and fear circuits and could potentially reveal a shared functional module for anxiety control similar to dSPN/iSPN dichotomy. Taken together, our results reveal that Co neurons, as an entire population, contribute to two sequential functions in the brain, firstly as guideposts and secondly as part of anxiety circuits. While the guidepost function is performed at earlier developmental stages, it is likely that their contribution to the extended amygdala constitutes their primary ancestral role (Bielle, Marcos-Mondéjar, et al., 2011; Bupesh et al., 2011; Medina, Bupesh, & Abellán, 2011). In addition, our work reveals unexpected ontogenic links between circuits and highlights the importance of tangential migration, thereby providing major insights for our understanding of normal and pathological wiring.

Acknowledgements

We are grateful to members of the Garel lab for discussions and inputs. We thank Christophe Auger, Déborah Souchet and Benjamin Mathieu for technical assistance. AT was supported by a doctoral fellowship from Boehringer Ingelheim Fonds and ENP. We are grateful to the IBENS Imaging Facility, which received the support of grants from the "Région Ile-de-France" (NERF N°2011-45), the "Fondation pour la Recherche Médicale" (N° DGE 20111123023), the "Fédération pour la Recherche sur le Cerveau - Rotary International France" (2011) and ANR-10-INSB-04-01 France-BioImaging infrastructure. A.N.R. was supported by a PhD studentship from the Wellcome Trust and funding in the N.K. lab was provided by an ERC Grant (207807). This work has received support under the program « Investissements d'Avenir » launched by the French Government and implemented by ANR with the references ANR–10–LABX–54 MEMOLIFE and ANR–10–IDEX–0001–02 PSL* Research University, as well as grants from the INSERM, CNRS, ANR Corridor and ERC NImO 616080 to S.G.. S.G is a member of the ENP.

Figure Legends

Figure 1. Tangentially oriented streams derive from LGE/CGE

(a-c) The Co is not derived from MGE/POA. (a) Schematic representation of *Nkx2.1cre* recombination pattern. (b) MGE/POA derived populations form the GP and contribute subset of cells to the Str, Co and neocortex (not shown); however, Islet1$^+$ Co neurons (labelled in magenta in c) are not derived from *Nkx2.1cre*+ progenitors. (**d**) Proposed migratory streams from MGE/POA. **(e-g)** Corridor cells derive from LGE/CGE. (e) Schematic representation of *Dlx1$^{fl/venus/fl}$* recombination pattern. (f-g) The Str (labelled in magenta by FoxP2 in g), Co and Vms are GFP$^+$ in E14 *Nkx2.1cre ;Dlx1$^{fl\text{-}Venus\text{-}fl}$* embryos, in which GFP expression is driven in cells derived from the LGE and CGE but not from MGE/POA. **(h)** Proposed migratory streams from LGE/CGE. **(i-i')** Str, Co and Vms cells are part of the *Nkx2.1*-negative *Islet1^{Cre}* domain. (**j-k)** Str, Co and Vms cells co-express Islet1 and Ebf1. Scale bars: 250 µm (b, f-g, i, j), 50 µm (c, i', k). CGE, caudal ganglionic eminence; Co, corridor; GP, globus– pallidus; LGE, lateral ganglionic eminence; MGE, medial ganglionic eminence; POA, preoptic area; Str, striatum; Vms, ventromedial stream.

Figure 2. Tangential streams include striatal-like *Drd2-EGFP*$^+$ neurons

(**a-a''**) In addition to Islet1$^+$ neurons (labelled in magenta in a-a''), Str, Co and Vms include a non-overlapping population of tangentially oriented *Drd2-EGFP*+ neurons (labelled in green in a'-a'') at E13.5. (**b-f**) *Drd2-EGFP*$^+$ neurons in Co have striatal-like molecular identity. At E13.5, *Drd2-EGFP*$^+$ neurons in both Str (b) and Co (b, c) co-express *Ctip2* (d; Str, 82±7% of *Drd2-EGFP*$^+$ cells, Co 91±6%, p>0.05) while they are not co-labelled by *Ebf1* (e-f; Str, 1±1% of *Drd2*-

EGFP$^+$ cells, Co 3±3%, p>0.05). These neurons are still present at E14.5 (**g-h**) and are negative for both Nkx2.1 (**i-i'**) and Prox1 (**j**, empty arrowheads indicate Prox1$^+$ cells), consistent with LGE/CGE origin. **(k-l')** Tangentially migrating cells from homotopic LGE explants. (k) Experimental procedure: explants of GFPu$^+$ LGE were taken from GFPu$^+$ coronal slices at E13.5 and grafted in the LGE of control (GFPu$^-$) littermates before culturing for 48h *in vitro* (hiv). (k') Tangential streams of migration originate from GFPu$^+$ LGE explants (full arrowhead) after 48hiv. (l) Experimental procedure: LGE explants was taken from *Drd2-EGFP*$^+$ coronal slices at E13.5 and grafted in the LGE of control (GFP$^-$) littermates before culturing for 48hiv. (l') GFP$^+$ cells migrate tangentially from *Drd2-EGFP*$^+$ explants after 48hiv. Scale bars: 250 µm (a-a'', b, e, g-g', i, k-l'), 50 µm (c, e', h, i, j). Co, corridor; GP, globus pallidus; LGE, lateral ganglionic eminence; MGE, medial ganglionic eminence; Str, striatum; Vms, ventromedial stream.

Figure 3. Co cells have molecular and cellular properties of projection neurons

(a-h) Co cells molecular fingerprint is related to, but different from striatal direct pathway neurons (dSPN). (**a**) At E13.5, both Str (b) and Co (c) contain *Islet1*^{Cre}*;R26*$^{YFP/+}$-Ctip2$^+$ double-positive neurons (d; Str, 93±2% of YFP$^+$ cells; Co, 77±14%; p>0.05). (e-h) However, while most *Islet1*^{Cre}*;R26*$^{YFP/+}$ cells co-express transcription factor FoxP1 in the Str (f, 71±9% of YFP$^+$ cells), Co cells do not (g, 5±4%), suggesting a distinct molecular identity of the two populations (h, p=0.002). (**i-n**) Co cells send early long-range projections. Either injection of AlexaFluor-coupled Cholera-ToxinB (CTB, n=4) at E12.5 (i-k) or DiI crystal insertion in the hypothalamus (l-n) at E14 (n=4) retro-label Islet1+ (k) and Ebf1+

(n) cell bodies, indicating that Co neurons extend axons outside of the telencephalon. Scale bars: 200 μm (a, e, m), 25 μm (b, c, e, f, g, j, n), 5 μm (k). Co, corridor; GP, globus pallidus; Str, striatum; Vms ventro-medial stream.

Figure 4. Corridor derivatives contribute to structures of the Central Extended Amygdala.

(a-d) *Islet1*-derived lineage participate to a continuum of structures, including striatum, Ipac and BNST. (a) X-gal staining of *Islet1^{Cre};R26$^{LacZ/+}$* cells at E18.5 shows a major contribution to the Str, BNST, and Ipac, as schematically represented in (b). (c-d) E18.5 *Nkx2.1cre; Dlx1$^{fl\text{-}Venus\text{-}fl}$* sections showing LGE/CGE contribution to BNST. **(e-f)** Conversely, only sparse *Nkx2.1cre; R26$^{LacZ/+}$* neurons are found in Str, BNST and Ipac, suggesting that central extended amygdala structures are mostly contributed by LGE/CGE-derived neurons. (**g-h**) Consistently, the BNST contains many GFP^{+} neurons in E18.5 *Nkx2.1cre; Dlx1$^{fl\text{-}Venus\text{-}fl}$* embryos, in which LGE/CGE-derived, but not MGE-derived neurons are labelled by GFP. **(i-j)** *In situ* hybridization at E18.5 showing contribution of *Ebf1*-expressing neurons to Str, BNST and Ipac. The BNST contains mostly early-born cells (**k,l**) and few late-born cells (**m**). **(n-u)** Islet1-derived cells of the BNST and IPAC have the same molecular fingerprint as Co cells. At E18.5 *Islet1^{Cre};R26^{YFP}* cells populating the BNST and the IPAC are double-positive for Ctip2 (n-q, BNST, 71±18%; IPAC, 69±10%) but do not express FoxP1 (r-u, BNST 11±10%, IPAC 7±3%). This molecular fingerprint is similar to Co and Vms cells, suggesting that the two populations contribute to the central extended amygdala. (**v-y**) The BNST (v,w) and the Ipac (x) contain also Drd2-EGFP^{+}; Ctip2^{+} double-positive neurons, consistent with the cellular

composition of Co and Vms streams (y, BNST 72±1%, IPAC 87±8%). Scale bars: 200 µm (a, c), 300 µm (e, f, i, j), 75 µm (g, h, k-m), 50 µm (e-g, i-k, m-o). Ac, anterior commissure; BNST, Bed nucleus of the stria terminalis; CeA, central extended amygdala; GP, globus pallidus; Ipac, interstitial nucleus of posterior limb of anterior commissure; Str, striatum.

Figure 5. Corridor derivatives contribute to Drd2-negative neurons in specific nuclei of the BNST

(**a**) Schematic representation of BNST main rostral subdivisions. (**b-b'''**) At P5, *Islet1*^{Cre}*;R26*$^{mt/+}$ (b) and Drd2-EGFP^{+} (b') cells are non-overlapping (b'') and intermixed (b''') in rostral BNST nuclei. (**c-g'**) At P14, Co derived neurons are still Ctip2^{+} (c-d) and FoxP1^{-} (e-f) and are unevenly distributed in rostral BNST, being prevalent in BNSTad and largely excluded from the BNSTov (g-g'). (**i-k**) Conversely, *Drd2-EGFP*$^{+}$ cells are scattered in BNSTad (i) and mostly participate to juBNST and BNSTov (k). (**h**) Schematic suggestion of LGE/CGE contribution to BNST nuclei and their possible functions, related to previously published results (H. W. Dong, Petrovich, & Swanson, 2001; Kim et al., 2013). Scale bars: 100 µm (b-b'', c-g, i-j), 25 µm (b''', g', k). ac, anterior commissure; ad, anterodorsal nucleus; BNST, bed nucleus of the stria terminalis; BS, brain stem; bTEL, basal telencephalon; dm, dorseomedial nucleus; HYP, hypothalamus; ju, juxtaposed nucleus; ov, ovalis nucleus; PB, parabrachial nucleus; Str, striatum; VTA, ventral tegmental area.

Figure 6. Defective corridor and reduced BNST size in *Ebf1* conditional knockout mice

(**a-b**) Expression pattern of Ebf1 protein in control (a) and *Dlx5/6::Cre; Ebf1*$^{fl/-}$ (cKO, b) embryos at E13.5 shows lack of Ebf1 protein in the cKO subapllium. (**c-f**) The shape of the Co and Vms is altered in *Ebf1* cKO. *In situ* hybridization with *Ebf1* full length probes recognizes all *Ebf1* transcripts, including the one generated by the floxed allele, thereby allowing the visualization of *Ebf1*-expressing cells in control and cKO context. At both E13.5 (c-d, n=3) and E14.5 (e-f, n=3) the shape of the Co and Vms is altered in *Ebf1* cKO. At E17.5 *Ebf1* transcripts are reduced in the cKO BNST (g-h, n=3), suggesting that less Co derivatives participate to this structure. (**i-k**) The size of the BNST is slightly reduced in *Ebf1* cKO (n=5) at P5 compared to controls (n=10), as shown by DAPI area measurement (79% of control BNST, Mann-Whitney U-value 13, $p<0.05$), indicating that corridor defect lead to defective BNST formation in *Ebf1* cKO. Scale bars: 200 µm (a-h), 300 µm (i-j). ac, anterior commissure; BNST, bed nucleus of stria terminalis; dBNST, dorsal BNST; Co, corridor; GP, globus pallidus; Ipac, interstitial nucleus of posterior limb of anterior commissure; Str, striatum; Vms, ventromedial stream.

Figure 7. Schematic representation of migratory streams in the subpallium

Integration into the currently established framework of migrations observed in the subpallium, from either the LGE/CGE or MGE and POA origins.

CGE, caudal ganglionic eminence; Co, corridor; GP, globus– pallidus; LGE, lateral ganglionic eminence; MGE, medial ganglionic eminence; POA, preoptic area; Str, striatum; Vms, ventromedial stream.

Bibliography

Ahmari, S. E., & Dougherty, D. D. (2015). DISSECTING OCD CIRCUITS: FROM ANIMAL MODELS TO TARGETED TREATMENTS. *Depression and Anxiety*, *32*(8), 550–562. https://doi.org/10.1002/da.22367

Alheid, G. F. (2003). Extended amygdala and basal forebrain. *Annals of the New York Academy of Sciences*, *985*, 185–205.

Arlotta, P., Molyneaux, B. J., Jabaudon, D., Yoshida, Y., & Macklis, J. D. (2008). Ctip2 Controls the Differentiation of Medium Spiny Neurons and the Establishment of the Cellular Architecture of the Striatum. *Journal of Neuroscience*, *28*(3), 622–632. https://doi.org/10.1523/JNEUROSCI.2986-07.2008

Asok, A., Schulkin, J., & Rosen, J. B. (2016). Corticotropin releasing factor type-1 receptor antagonism in the dorsolateral bed nucleus of the stria terminalis disrupts contextually conditioned fear, but not unconditioned fear to a predator odor. *Psychoneuroendocrinology*, *70*, 17–24. https://doi.org/10.1016/j.psyneuen.2016.04.021

Bayer, S. A. (1987). Neurogenetic and morphogenetic heterogeneity in the bed nucleus of the stria terminalis. *The Journal of Comparative Neurology*, *265*(1), 47–64. https://doi.org/10.1002/cne.902650105

Bielle, F., Marcos-Mondejar, P., Keita, M., Mailhes, C., Verney, C., Nguyen Ba-Charvet, K., … Garel, S. (2011). Slit2 Activity in the Migration of Guidepost Neurons Shapes Thalamic Projections during Development and Evolution. *Neuron*, *69*(6), 1085–1098. https://doi.org/10.1016/j.neuron.2011.02.026

Bielle, F., Marcos-Mondéjar, P., Leyva-Díaz, E., Lokmane, L., Mire, E., Mailhes, C., … López-Bendito, G. (2011). Emergent growth cone responses to combinations of Slit1 and Netrin 1 in thalamocortical axon topography. *Current Biology: CB*, *21*(20), 1748–1755. https://doi.org/10.1016/j.cub.2011.09.008

Bodnar, R. J. (2013). Endogenous opiates and behavior: 2012. *Peptides*, *50*, 55–95. https://doi.org/10.1016/j.peptides.2013.10.001

Brown, M. T. C., Tan, K. R., O'Connor, E. C., Nikonenko, I., Muller, D., & Lüscher, C. (2012). Ventral tegmental area GABA projections pause accumbal cholinergic interneurons to enhance associative learning. *Nature*, *advance online publication*. https://doi.org/10.1038/nature11657

Bupesh, M., Abellán, A., & Medina, L. (2011). Genetic and experimental evidence supports the continuum of the central extended amygdala and a mutiple embryonic origin of its principal neurons. *The Journal of Comparative Neurology*, *519*(17), 3507–3531. https://doi.org/10.1002/cne.22719

Cai, H., Haubensak, W., Anthony, T. E., & Anderson, D. J. (2014). Central amygdala PKC-δ(+) neurons mediate the influence of multiple anorexigenic signals. *Nature Neuroscience*, *17*(9), 1240–1248. https://doi.org/10.1038/nn.3767

Chen, Y.-C., Kuo, H.-Y., Bornschein, U., Takahashi, H., Chen, S.-Y., Lu, K.-M., … Liu, F.-C. (2016). Foxp2 controls synaptic wiring of corticostriatal circuits and vocal communication by opposing Mef2c. *Nature Neuroscience*, *19*(11), 1513–1522. https://doi.org/10.1038/nn.4380

Chiu, Y.-C., Li, M.-Y., Liu, Y.-H., Ding, J.-Y., Yu, J.-Y., & Wang, T.-W. (2014). Foxp2 regulates neuronal differentiation and neuronal subtype specification. *Developmental Neurobiology*, *74*(7), 723–738. https://doi.org/10.1002/dneu.22166

Choi, D. C., Furay, A. R., Evanson, N. K., Ostrander, M. M., Ulrich-Lai, Y. M., & Herman, J. P. (2007). Bed nucleus of the stria terminalis subregions differentially regulate hypothalamic-pituitary-adrenal axis activity: implications for the integration of limbic inputs. *The Journal of Neuroscience: The Official Journal of the Society for Neuroscience*, *27*(8), 2025–2034. https://doi.org/10.1523/JNEUROSCI.4301-06.2007

Ciceri, G., Dehorter, N., Sols, I., Huang, Z. J., Maravall, M., & Marín, O. (2013). Lineage-specific laminar organization of cortical GABAergic interneurons. *Nature Neuroscience*, *16*(9), 1199–1210. https://doi.org/10.1038/nn.3485

Corbin, J. G., & Butt, S. J. B. (2011). Developmental mechanisms for the generation of telencephalic interneurons. *Developmental Neurobiology*, *71*(8), 710–732. https://doi.org/10.1002/dneu.20890

Corbin, J. G., Nery, S., & Fishell, G. (2001). Telencephalic cells take a tangent: non-radial migration in the mammalian forebrain. *Nature Neuroscience*, *4 Suppl*, 1177–1182. https://doi.org/10.1038/nn749

Crowley, N. A., Bloodgood, D. W., Hardaway, J. A., Kendra, A. M., McCall, J. G., Al-Hasani, R., … Kash, T. L. (2016). Dynorphin Controls the Gain of an Amygdalar Anxiety Circuit. *Cell Reports*, *14*(12), 2774–2783. https://doi.org/10.1016/j.celrep.2016.02.069

Daldrup, T., Lesting, J., Meuth, P., Seidenbecher, T., & Pape, H.-C. (2016). Neuronal correlates of sustained fear in the anterolateral part of the bed

nucleus of stria terminalis. *Neurobiology of Learning and Memory*, *131*, 137–146. https://doi.org/10.1016/j.nlm.2016.03.020

de Frutos, C. A., Bouvier, G., Arai, Y., Thion, M. S., Lokmane, L., Keita, M., … Garel, S. (2016). Reallocation of Olfactory Cajal-Retzius Cells Shapes Neocortex Architecture. *Neuron*, *92*(2), 435–448. https://doi.org/10.1016/j.neuron.2016.09.020

de Olmos, J. S., & Heimer, L. (1999). The concepts of the ventral striatopallidal system and extended amygdala. *Annals of the New York Academy of Sciences*, *877*, 1–32.

Deng, Y.-P., Wong, T., Wan, J. Y., & Reiner, A. (2014). Differential loss of thalamostriatal and corticostriatal input to striatal projection neuron types prior to overt motor symptoms in the Q140 knock-in mouse model of Huntington's disease. *Frontiers in Systems Neuroscience*, *8*, 198. https://doi.org/10.3389/fnsys.2014.00198

Dodson, P. D., Larvin, J. T., Duffell, J. M., Garas, F. N., Doig, N. M., Kessaris, N., … Magill, P. J. (2015). Distinct Developmental Origins Manifest in the Specialized Encoding of Movement by Adult Neurons of the External Globus Pallidus. *Neuron*, *86*(2), 501–513. https://doi.org/10.1016/j.neuron.2015.03.007

Dong, H. W., Petrovich, G. D., & Swanson, L. W. (2001). Topography of projections from amygdala to bed nuclei of the stria terminalis. *Brain Research. Brain Research Reviews*, *38*(1–2), 192–246.

Dong, H.-W., & Swanson, L. W. (2004). Organization of axonal projections from the anterolateral area of the bed nuclei of the stria terminalis. *The*

Journal of Comparative Neurology, *468*(2), 277–298. https://doi.org/10.1002/cne.10949

Ehrman, L. A., Mu, X., Waclaw, R. R., Yoshida, Y., Vorhees, C. V., Klein, W. H., & Campbell, K. (2013). The LIM homeobox gene Isl1 is required for the correct development of the striatonigral pathway in the mouse. *Proceedings of the National Academy of Sciences*, *110*(42), E4026–E4035. https://doi.org/10.1073/pnas.1308275110

Eisenstat, D. D., Liu, J. K., Mione, M., Zhong, W., Yu, G., Anderson, S. A., … Rubenstein, J. L. (1999). DLX-1, DLX-2, and DLX-5 expression define distinct stages of basal forebrain differentiation. *Journal of Comparative Neurology*, *414*(2), 217–237.

Elshatory, Y., & Gan, L. (2008). The LIM-homeobox gene Islet-1 is required for the development of restricted forebrain cholinergic neurons. *The Journal of Neuroscience: The Official Journal of the Society for Neuroscience*, *28*(13), 3291–3297. https://doi.org/10.1523/JNEUROSCI.5730-07.2008

Enard, W. (2011). FOXP2 and the role of cortico-basal ganglia circuits in speech and language evolution. *Current Opinion in Neurobiology*, *21*(3), 415–424. https://doi.org/10.1016/j.conb.2011.04.008

Enard, W., Gehre, S., Hammerschmidt, K., Hölter, S. M., Blass, T., Somel, M., … Pääbo, S. (2009). A humanized version of Foxp2 affects cortico-basal ganglia circuits in mice. *Cell*, *137*(5), 961–971. https://doi.org/10.1016/j.cell.2009.03.041

Feng, J., Xian, Q., Guan, T., Hu, J., Wang, M., Huang, Y., … Zhou, L. (2016). Celsr3 and Fzd3 Organize a Pioneer Neuron Scaffold to Steer Growing

Thalamocortical Axons. *Cerebral Cortex (New York, N.Y.: 1991)*, *26*(7), 3323–3334. https://doi.org/10.1093/cercor/bhw132

Ferland, R. J., Cherry, T. J., Preware, P. O., Morrisey, E. E., & Walsh, C. A. (2003). Characterization of Foxp2 and Foxp1 mRNA and protein in the developing and mature brain. *The Journal of Comparative Neurology*, *460*(2), 266–279. https://doi.org/10.1002/cne.10654

Garcia-Calero, E., Botella-Lopez, A., Bahamonde, O., Perez-Balaguer, A., & Martinez, S. (2015). FoxP2 protein levels regulate cell morphology changes and migration patterns in the vertebrate developing telencephalon. *Brain Structure & Function*. https://doi.org/10.1007/s00429-015-1079-7

Garel, S., & López-Bendito, G. (2014). Inputs from the thalamocortical system on axon pathfinding mechanisms. *Current Opinion in Neurobiology*, *27*, 143–150. https://doi.org/10.1016/j.conb.2014.03.013

Garel, S., Marín, F., Grosschedl, R., & Charnay, P. (1999). Ebf1 controls early cell differentiation in the embryonic striatum. *Development*, *126*(23), 5285–5294.

Garel, S., Yun, K., Grosschedl, R., & Rubenstein, J. L. R. (2002). The early topography of thalamocortical projections is shifted in *Ebf1* and *Dlx1/2* mutant mice. *Development*, *129*(24), 5621–5634. https://doi.org/10.1242/dev.00166

Gelman, D. M., Marín;, O., & Rubenstein, J. L. R. (2012). The Generation of Cortical Interneurons. In J. L. Noebels, M. Avoli, M. A. Rogawski, R. W. Olsen, & A. V. Delgado-Escueta (Eds.), *Jasper's Basic Mechanisms of the Epilepsies* (4th ed.). Bethesda (MD): National Center for

Biotechnology Information (US). Retrieved from http://www.ncbi.nlm.nih.gov/books/NBK98190/

Geng, F., Zhang, J., Wu, J.-L., Zou, W.-J., Liang, Z.-P., Bi, L.-L., … Gao, T.-M. (2016). Neuregulin 1-ErbB4 signaling in the bed nucleus of the stria terminalis regulates anxiety-like behavior. *Neuroscience*, *329*, 182–192. https://doi.org/10.1016/j.neuroscience.2016.05.018

Gong, S., Zheng, C., Doughty, M. L., Losos, K., Didkovsky, N., Schambra, U. B., … Heintz, N. (2003). A gene expression atlas of the central nervous system based on bacterial artificial chromosomes. *Nature*, *425*(6961), 917–925. https://doi.org/10.1038/nature02033

Grant, E., Hoerder-Suabedissen, A., & Molnár, Z. (2012). Development of the Corticothalamic Projections. *Frontiers in Neuroscience*, *6*. https://doi.org/10.3389/fnins.2012.00053

Hagimoto, K., Takami, S., Murakami, F., & Tanabe, Y. (2017). Distinct migratory behaviors of striosome and matrix cells underlying the mosaic formation in the developing striatum. *Journal of Comparative Neurology*, *525*(4), 794–817. https://doi.org/10.1002/cne.24096

Halliday, A. L., & Cepko, C. L. (1992). Generation and migration of cells in the developing striatum. *Neuron*, *9*(1), 15–26. https://doi.org/10.1016/0896-6273(92)90216-Z

Hamasaki, T., Goto, S., Nishikawa, S., & Ushio, Y. (2003). Neuronal cell migration for the developmental formation of the mammalian striatum. *Brain Research Reviews*, *41*(1), 1–12.

Haubensak, W., Kunwar, P. S., Cai, H., Ciocchi, S., Wall, N. R., Ponnusamy, R., … Anderson, D. J. (2010). Genetic dissection of an amygdala

microcircuit that gates conditioned fear. *Nature*, *468*(7321), 270–276. https://doi.org/10.1038/nature09553

Heimer, L., Van Hoesen, G.W., Trimble, M., & Zahm, D.S. (2008) Cooperation and competition of macrosystem outputs. Anatomy of Neuropsychiatry, Chapter 5, Elsevier.

Hirata, T., Li, P., Lanuza, G. M., Cocas, L. A., Huntsman, M. M., & Corbin, J. G. (2009). Identification of distinct telencephalic progenitor pools for neuronal diversity in the amygdala. *Nature Neuroscience*, *12*(2), 141–149. https://doi.org/10.1038/nn.2241

Hott, S. C., Gomes, F. V., Uliana, D. L., Vale, G. T., Tirapelli, C. R., & Resstel, L. B. M. (2016). Bed nucleus of the stria terminalis NMDA receptors and nitric oxide modulate contextual fear conditioning in rats. *Neuropharmacology*. https://doi.org/10.1016/j.neuropharm.2016.05.022

Ju, G., & Han, Z. S. (1989). Coexistence of corticotropin releasing factor and neurotensin within oval nucleus neurons in the bed nuclei of the stria terminalis in the rat. *Neuroscience Letters*, *99*(3), 246–250.

Kessaris, N., Magno, L., Rubin, A. N., & Oliveira, M. G. (2014). Genetic programs controlling cortical interneuron fate. *Current Opinion in Neurobiology*, *26*, 79–87. https://doi.org/10.1016/j.conb.2013.12.012

Kim, S.-Y., Adhikari, A., Lee, S. Y., Marshel, J. H., Kim, C. K., Mallory, C. S., … Deisseroth, K. (2013). Diverging neural pathways assemble a behavioural state from separable features in anxiety. *Nature*, *496*(7444), 219–223. https://doi.org/10.1038/nature12018

Lemon, R. N. (2008). Descending Pathways in Motor Control. *Annual Review of Neuroscience*, *31*(1), 195–218. https://doi.org/10.1146/annurev.neuro.31.060407.125547

Lobo, M. K., Karsten, S. L., Gray, M., Geschwind, D. H., & Yang, X. W. (2006). FACS-array profiling of striatal projection neuron subtypes in juvenile and adult mouse brains. *Nature Neuroscience*, *9*(3), 443–452. https://doi.org/10.1038/nn1654

Lobo, M. K., Yeh, C., & Yang, X. W. (2008). Pivotal role of early B-cell factor 1 in development of striatonigral medium spiny neurons in the matrix compartment. *Journal of Neuroscience Research*, *86*(10), 2134–2146. https://doi.org/10.1002/jnr.21666

Lokmane, L., & Garel, S. (2014). Map transfer from the thalamus to the neocortex: inputs from the barrel field. *Seminars in Cell & Developmental Biology*, *35*, 147–155. https://doi.org/10.1016/j.semcdb.2014.07.005

Lokmane, L., Proville, R., Narboux-Nême, N., Györy, I., Keita, M., Mailhes, C., … Garel, S. (2013). Sensory Map Transfer to the Neocortex Relies on Pretarget Ordering of Thalamic Axons. *Current Biology*, *23*(9), 810–816. https://doi.org/10.1016/j.cub.2013.03.062

Long, J. E., Cobos, I., Potter, G. B., & Rubenstein, J. L. R. (2009). Dlx1&2 and Mash1 Transcription Factors Control MGE and CGE Patterning and Differentiation through Parallel and Overlapping Pathways. *Cerebral Cortex (New York, NY)*, *19*(Suppl 1), i96–i106. https://doi.org/10.1093/cercor/bhp045

López-Bendito, G., Cautinat, A., Sánchez, J. A., Bielle, F., Flames, N., Garratt, A. N., … Garel, S. (2006). Tangential Neuronal Migration Controls Axon

Guidance: A Role for Neuregulin-1 in Thalamocortical Axon Navigation. *Cell*, *125*(1), 127–142. https://doi.org/10.1016/j.cell.2006.01.042

Lu, K.-M., Evans, S. M., Hirano, S., & Liu, F.-C. (2014). Dual role for Islet-1 in promoting striatonigral and repressing striatopallidal genetic programs to specify striatonigral cell identity. *Proceedings of the National Academy of Sciences*, *111*(1), E168–E177. https://doi.org/10.1073/pnas.1319138111

Marin, O., Anderson, S. A., & Rubenstein, J. L. (2000). Origin and molecular specification of striatal interneurons. *The Journal of Neuroscience: The Official Journal of the Society for Neuroscience*, *20*(16), 6063–6076.

Marín, O., & Rubenstein, J. L. (2001). A long, remarkable journey: tangential migration in the telencephalon. *Nature Reviews Neuroscience*, *2*(11), 780–790.

Marín, O., & Rubenstein, J. L. R. (2003). Cell migration in the forebrain. *Annual Review of Neuroscience*, *26*(1), 441–483. https://doi.org/10.1146/annurev.neuro.26.041002.131058

Medina, L., Bupesh, M., & Abellán, A. (2011). Contribution of Genoarchitecture to Understanding Forebrain Evolution and Development, with Particular Emphasis on the Amygdala. *Brain, Behavior and Evolution*, *78*(3), 216–236. https://doi.org/10.1159/000330056

Miyoshi, G., Young, A., Petros, T., Karayannis, T., McKenzie Chang, M., Lavado, A., … Fishell, G. (2015). Prox1 Regulates the Subtype-Specific Development of Caudal Ganglionic Eminence-Derived GABAergic Cortical Interneurons. *The Journal of Neuroscience: The Official Journal of the Society for Neuroscience*, *35*(37), 12869–12889. https://doi.org/10.1523/JNEUROSCI.1164-15.2015

Molnár, Z., Garel, S., López-Bendito, G., Maness, P., & Price, D. J. (2012). Mechanisms controlling the guidance of thalamocortical axons through the embryonic forebrain. *The European Journal of Neuroscience*, *35*(10), 1573–1585. https://doi.org/10.1111/j.1460-9568.2012.08119.x

Morano, T. J., Bailey, N. J., Cahill, C. M., & Dumont, E. C. (2008). Nuclei-and condition-specific responses to pain in the bed nucleus of the stria terminalis. *Progress in Neuro-Psychopharmacology & Biological Psychiatry*, *32*(3), 643–650. https://doi.org/10.1016/j.pnpbp.2007.11.003

Morello, F., Prasad, A. A., Rehberg, K., Vieira de Sá, R., Antón-Bolaños, N., Leyva-Diaz, E., … Pasterkamp, R. J. (2015). Frizzled3 Controls Axonal Polarity and Intermediate Target Entry during Striatal Pathway Development. *The Journal of Neuroscience: The Official Journal of the Society for Neuroscience*, *35*(42), 14205–14219. https://doi.org/10.1523/JNEUROSCI.1840-15.2015

Nóbrega-Pereira, S., Gelman, D., Bartolini, G., Pla, R., Pierani, A., & Marín, O. (2010). Origin and molecular specification of globus pallidus neurons. *The Journal of Neuroscience: The Official Journal of the Society for Neuroscience*, *30*(8), 2824–2834. https://doi.org/10.1523/JNEUROSCI.4023-09.2010

Nóbrega-Pereira, S., Kessaris, N., Du, T., Kimura, S., Anderson, S. A., & Marín, O. (2008). Postmitotic Nkx2-1 controls the migration of telencephalic interneurons by direct repression of guidance receptors. *Neuron*, *59*(5), 733–745. https://doi.org/10.1016/j.neuron.2008.07.024

Olmos, J. L., Real, M. A., Medina, L., Guirado, S., & Dávila, J. C. (2005). Distribution of nitric oxide-producing neurons in the developing and adult

mouse amygdalar basolateral complex. *Brain Research Bulletin*, *66*(4–6), 465–469. https://doi.org/10.1016/j.brainresbull.2005.04.002

Pêgo, J. M., Morgado, P., Pinto, L. G., Cerqueira, J. J., Almeida, O. F. X., & Sousa, N. (2008). Dissociation of the morphological correlates of stress-induced anxiety and fear. *The European Journal of Neuroscience*, *27*(6), 1503–1516. https://doi.org/10.1111/j.1460-9568.2008.06112.x

Ranjan, V., Singh, S., Siddiqui, S. A., Tripathi, S., Khan, M. Y., & Prakash, A. (2017). Differential Histone Acetylation in Sub-Regions of Bed Nucleus of the Stria Terminalis Underlies Fear Consolidation and Extinction. *Psychiatry Investigation*, *14*(3), 350–359. https://doi.org/10.4306/pi.2017.14.3.350

Reiner, A. (2010). Corticostriatal projection neurons – dichotomous types and dichotomous functions. *Frontiers in Neuroanatomy*, *4*. https://doi.org/10.3389/fnana.2010.00142

Rubin, A. N., Alfonsi, F., Humphreys, M. P., Choi, C. K. P., Rocha, S. F., & Kessaris, N. (2010). The germinal zones of the basal ganglia but not the septum generate GABAergic interneurons for the cortex. *The Journal of Neuroscience: The Official Journal of the Society for Neuroscience*, *30*(36), 12050–12062. https://doi.org/10.1523/JNEUROSCI.6178-09.2010

Rubin, A. N., & Kessaris, N. (2013). PROX1: a lineage tracer for cortical interneurons originating in the lateral/caudal ganglionic eminence and preoptic area. *PloS One*, *8*(10), e77339. https://doi.org/10.1371/journal.pone.0077339

Sherman, S. M. (2016). Thalamus plays a central role in ongoing cortical functioning. *Nature Neuroscience*, *19*(4), 533–541. https://doi.org/10.1038/nn.4269

Sippy, T., Lapray, D., Crochet, S., & Petersen, C. C. H. (2015). Cell-Type-Specific Sensorimotor Processing in Striatal Projection Neurons during Goal-Directed Behavior. *Neuron*, *88*(2), 298–305. https://doi.org/10.1016/j.neuron.2015.08.039

Squarzoni, P., Thion, M. S., & Garel, S. (2015). Neuronal and microglial regulators of cortical wiring: usual and novel guideposts. *Frontiers in Neuroscience*, *9*, 248. https://doi.org/10.3389/fnins.2015.00248

Srinivas, S., Watanabe, T., Lin, C. S., William, C. M., Tanabe, Y., Jessell, T. M., & Costantini, F. (2001). Cre reporter strains produced by targeted insertion of EYFP and ECFP into the ROSA26 locus. *BMC Developmental Biology*, *1*, 4.

Taverna, S., Ilijic, E., & Surmeier, D. J. (2008). Recurrent Collateral Connections of Striatal Medium Spiny Neurons Are Disrupted in Models of Parkinson's Disease. *Journal of Neuroscience*, *28*(21), 5504–5512. https://doi.org/10.1523/JNEUROSCI.5493-07.2008

Torigoe, M., Yamauchi, K., Kimura, T., Uemura, Y., & Murakami, F. (2016). Evidence That the Laminar Fate of LGE/CGE-Derived Neocortical Interneurons Is Dependent on Their Progenitor Domains. *The Journal of Neuroscience: The Official Journal of the Society for Neuroscience*, *36*(6), 2044–2056. https://doi.org/10.1523/JNEUROSCI.3550-15.2016

Touzot, A., Ruiz-Reig, N., Vitalis, T., & Studer, M. (2016). Molecular control of two novel migratory paths for CGE-derived interneurons in the

developing mouse brain. *Development*, *143*(10), 1753–1765. https://doi.org/10.1242/dev.131102

Tovote, P., Fadok, J. P., & Lüthi, A. (2015). Neuronal circuits for fear and anxiety. *Nature Reviews. Neuroscience*, *16*(6), 317–331. https://doi.org/10.1038/nrn3945

Ventura-Silva, A. P., Pêgo, J. M., Sousa, J. C., Marques, A. R., Rodrigues, A. J., Marques, F., … Sousa, N. (2012). Stress shifts the response of the bed nucleus of the stria terminalis to an anxiogenic mode. *The European Journal of Neuroscience*, *36*(10), 3396–3406. https://doi.org/10.1111/j.1460-9568.2012.08262.x

Waclaw, R. R., Ehrman, L. A., Pierani, A., & Campbell, K. (2010). Developmental Origin of the Neuronal Subtypes That Comprise the Amygdalar Fear Circuit in the Mouse. *Journal of Neuroscience*, *30*(20), 6944–6953. https://doi.org/10.1523/JNEUROSCI.5772-09.2010

Walker, D. L., & Davis, M. (2008). Role of the extended amygdala in short-duration versus sustained fear: a tribute to Dr. Lennart Heimer. *Brain Structure & Function*, *213*(1–2), 29–42. https://doi.org/10.1007/s00429-008-0183-3

Wall, N. R., De La Parra, M., Callaway, E. M., & Kreitzer, A. C. (2013). Differential Innervation of Direct- and Indirect-Pathway Striatal Projection Neurons. *Neuron*, *79*(2), 347–360. https://doi.org/10.1016/j.neuron.2013.05.014

Waraczynski, M. A. (2006). The central extended amygdala network as a proposed circuit underlying reward valuation. *Neuroscience and*

Biobehavioral Reviews, *30*(4), 472–496. https://doi.org/10.1016/j.neubiorev.2005.09.001

Wichterle, H., Turnbull, D. H., Nery, S., Fishell, G., & Alvarez-Buylla, A. (2001). In utero fate mapping reveals distinct migratory pathways and fates of neurons born in the mammalian basal forebrain. *Development*, *128*(19), 3759–3771.

Xu, Q., Tam, M., & Anderson, S. A. (2008). Fate mapping Nkx2.1-lineage cells in the mouse telencephalon. *The Journal of Comparative Neurology*, *506*(1), 16–29. https://doi.org/10.1002/cne.21529

Yun, K., Fischman, S., Johnson, J., de Angelis, M. H., Weinmaster, G., & Rubenstein, J. L. (2002). Modulation of the notch signaling by Mash1 and Dlx1/2 regulates sequential specification and differentiation of progenitor cell types in the subcortical telencephalon. *Development*, *129*(21), 5029–5040.

Zerucha, T., Stühmer, T., Hatch, G., Park, B. K., Long, Q., Yu, G., … Ekker, M. (2000). A Highly Conserved Enhancer in the Dlx5/Dlx6Intergenic Region is the Site of Cross-Regulatory Interactions betweenDlx Genes in the Embryonic Forebrain. *Journal of Neuroscience*, *20*(2), 709–721.

Zhou, L., Qu, Y., Tissir, F., & Goffinet, A. M. (2009). Role of the atypical cadherin Celsr3 during development of the internal capsule. *Cerebral Cortex (New York, N.Y.: 1991)*, *19 Suppl 1*, i114-119. https://doi.org/10.1093/cercor/bhp032

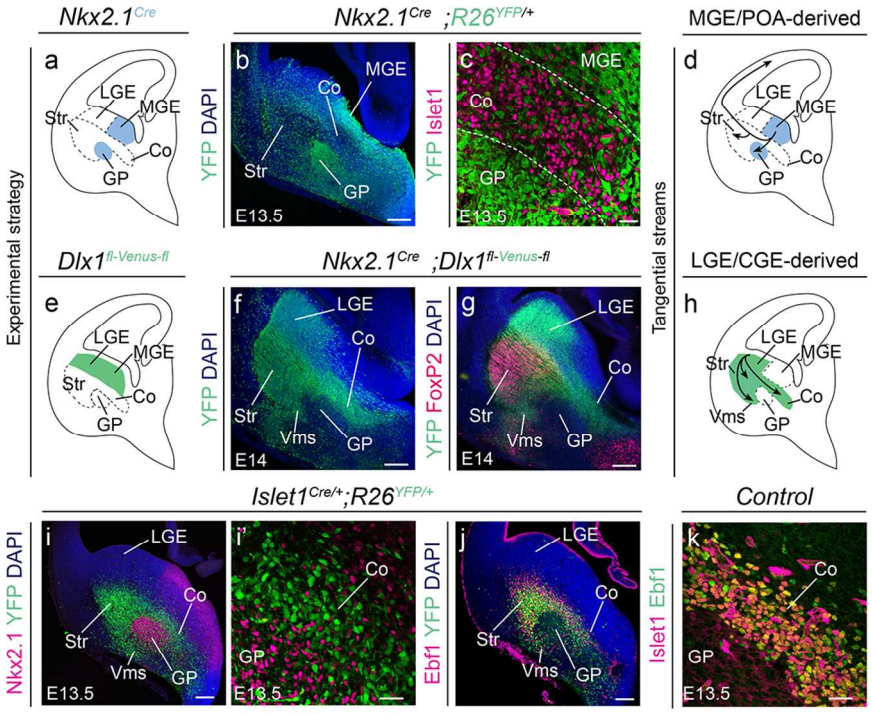

Figure 1

Tinterri et al.

Figure 1 Revised (Magenta/Green)

99x132mm (300 x 300 DPI)

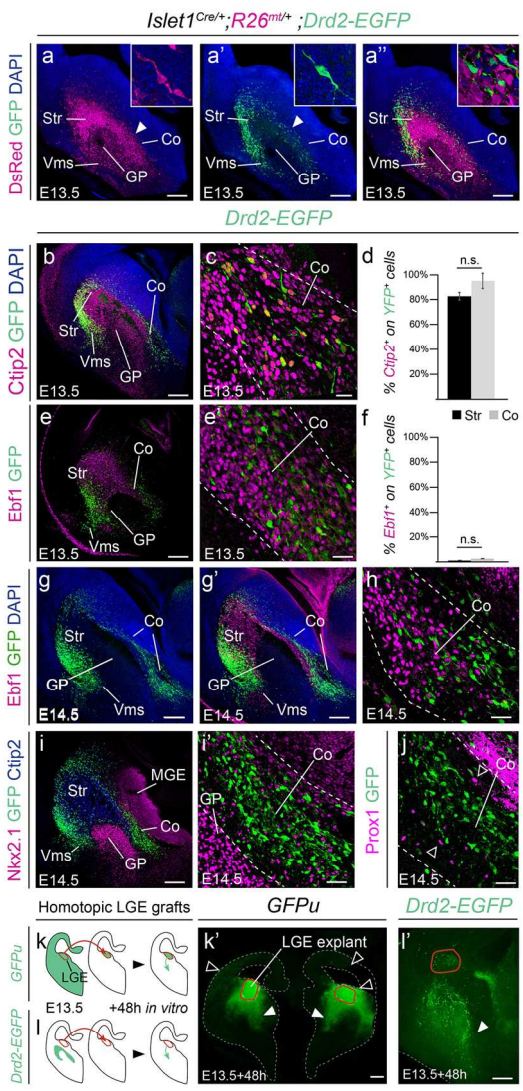

Figure 2

Tinterri et al.

Figure 2 Revised (Magenta/Green)

90x195mm (300 x 300 DPI)

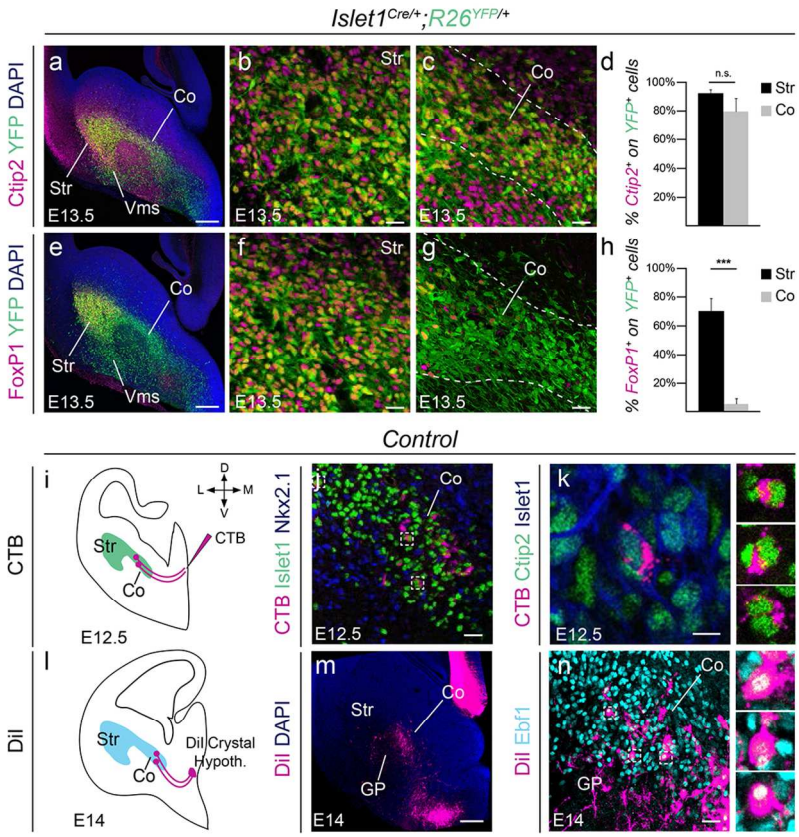

Figure 3

Tinterri et al.

Figure 3 Revised (Magenta/Green)

99x144mm (300 x 300 DPI)

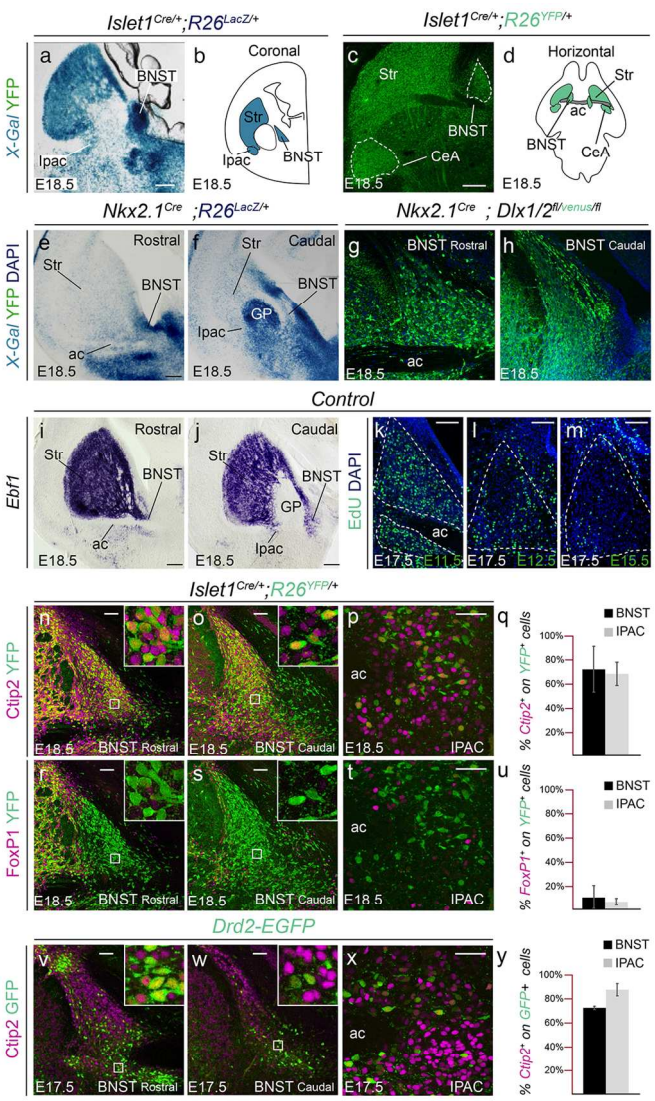

Figure 4
Tinterri et al.

Figure 4 Revised (Magenta/Green)

99x176mm (300 x 300 DPI)

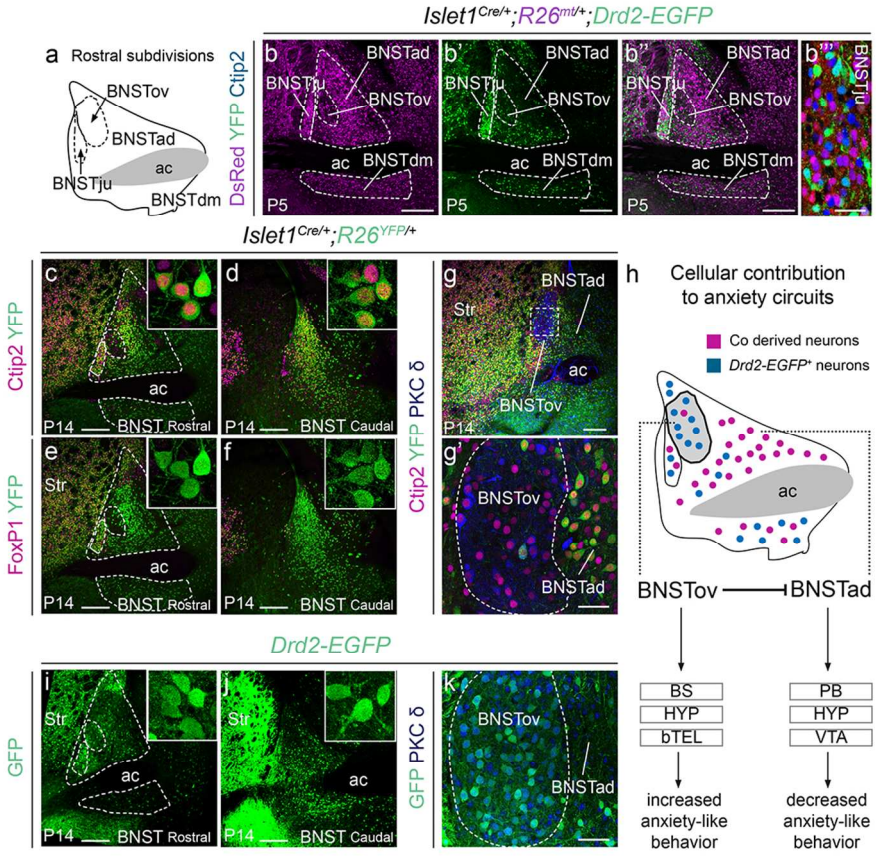

Figure 5

Tinterri et al.

Figure 5 Revised (Magenta/Green)

99x131mm (300 x 300 DPI)

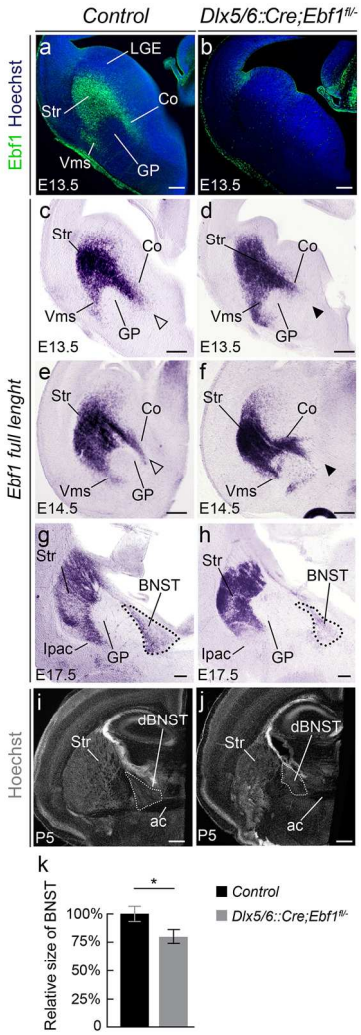

Figure 6
Tinterri et al.

Figure 6 Revised

65x206mm (300 x 300 DPI)

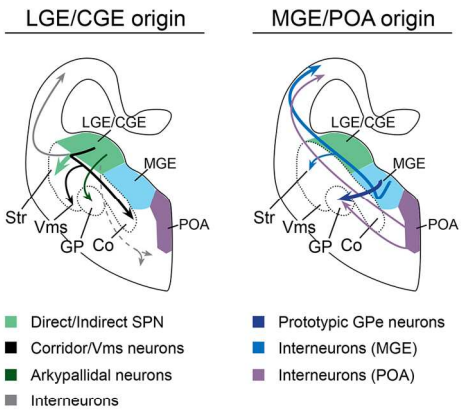

Figure 7
Tinterri et al.

Figure 7 Revised

80x190mm (300 x 300 DPI)

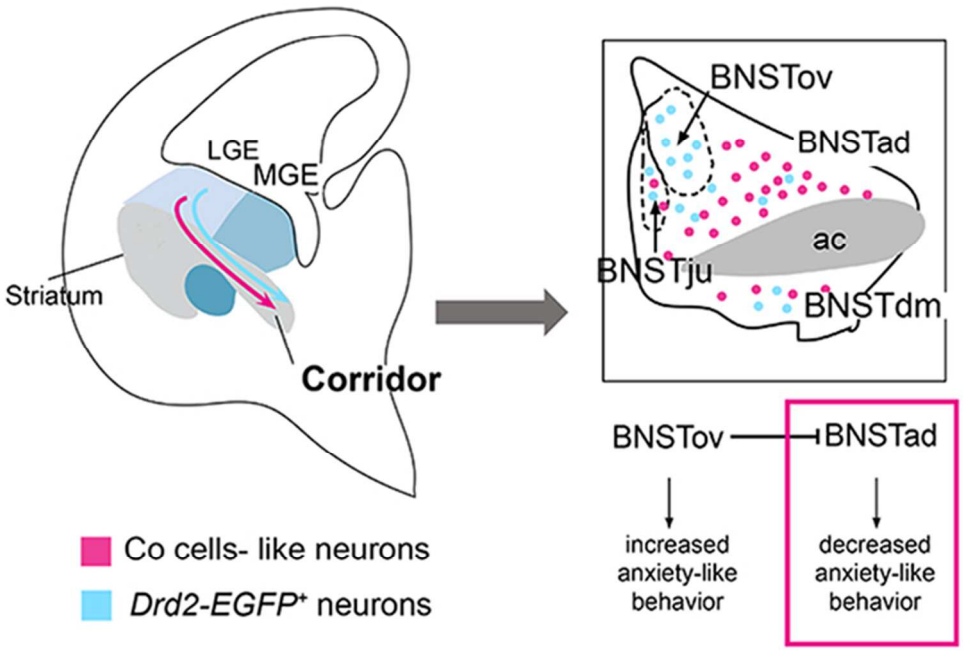

60x50mm (300 x 300 DPI)

Here, we investigated the contribution of corridor (Co) cells, which migrate in the embryonic subpallium, to mature brain circuits using a combination of genetic fate-mapping and assays in mice. We unexpectedly found that Co neurons contribute to striatal-like projection neurons in specific nuclei of the central extended amygdala, including the Bed Nucleus of the Stria Terminalis (BNST).